Stochastic Geometry-Based Performance Analysis of Cellular Systems in the Vicinity of Rotating Radars

Mai Kafafy, Ahmed S. Ibrahim, *Member, IEEE*, and Mahmoud H. Ismail, *Senior Member, IEEE*

***Abstract*— This letter analyzes the performance of a cellular system that shares spectrum with a nearby rotating radar. The analysis is based on stochastic geometry and combines opportunistic with concurrent spectrum sharing. We derive expressions for the cellular probability of coverage taking into consideration the radar guard zone and the operating parameters of both the radar and the cellular system. Results show that allowing eNBs inside the radar guard zone to operate when not in the radar beam improves the coverage and service of the cellular system compared to the case of a strictly silent guard zone.**

***Index Terms*— Spectrum sharing, radar, stochastic geometry, performance evaluation.**

I. Introduction

SPECTRUM sharing between radars and cellular systems is a promising solution to relieve the congested RF spectrum. Nevertheless, it should be regulated in order not to compromise the performance of the primary occupant, the radar in this case. Spectrum sharing has two models: opportunistic and concurrent [1]. Opportunistic sharing allows the secondary system to use the spectrum only when it is not used by the primary occupant while concurrent sharing allows both systems to access the spectrum under interference constraints. Different aspects of coexistence between wireless communication and radars have been investigated in the literature. For example, the feasibility of spectrum sharing between radars and LTE was verified through simulations in [2] and [3]. Reference [2] considered a single LTE eNodeB (eNB) operating in the presence of an air traffic control radar, while [3] considered an LTE system operating in the presence of a rotating shipborne radar. Furthermore, power control was used in [4]–[6] to allow spectrum sharing without harming the radar operation. In addition, [4] considered a simple model of a single eNB with a single user where the eNB adjusts its transmission power based on the antenna direction of a rotating radar while [5] considered multiple eNBs and a shipborne radar with a fixed antenna position. It proposed an iterative algorithm that increments the transmission powers of the eNBs, starting from the farthest to the radar, until an interference threshold is violated. However, it did not evaluate the effect of that power control on the cellular system performance. Similarly, [6] considered multiple eNBs and a tracking radar with unknown antenna direction, and the transmission power of a single eNB was maximized given its distance from the radar. The power control had constraints on the radar outage and the worst case communication outage of a cell edge user in the radar beam. Also, the authors in [7] calculated the minimum guard distance required to protect a radar from a WiFi system, given the radiation pattern of its antenna. They considered the cases when the WiFi access points have full knowledge, partial knowledge, or no knowledge of the radar antenna direction and evaluated, through simulations, the WiFi throughput for those cases. Although [6] and [7] assumed randomly located eNBs/access points when evaluating the radar performance, they evaluated the cellular system performance for a single user at specific location relative to the radar and to its serving eNB assuming zero inter-eNB interference. The single-cell approach in [6], [7] suits communication hotspots that experience low interference and whose users are clustered within a specific radius. However, evaluating the performance of a general cellular system in the presence of a radar needs a more general stochastic framework that captures the uncertainties in the numbers and locations of both the users and the eNBs besides the uncertainty in the distance between each user and its serving eNB.

In this letter, we consider hybrid spectrum sharing such that eNBs inside the radar guard zone share the radar spectrum only when not in the radar beam (i.e., spatial opportunistic sharing) while eNBs outside the guard zone share the radar spectrum all the time (i.e., concurrent sharing). Our contributions are summarized as follows:

- To the best of our knowledge, this is the first stochastic geometry based performance analysis of a cellular system under hybrid spectrum sharing with a rotating radar. The analysis is challenging due to the radar rotation and the presence of a guard zone, which affects the spectrum sharing pattern of eNBs and the observed radar/cellular interference. Also, the randomness in the number and positions of eNBs and users adds uncertainty to the spectrum sharing model with which a user is served.
- We derive expressions, with closed-form approximations, for the probability of coverage for the two cases when spatial opportunistic spectrum sharing is allowed inside

Manuscript received November 21, 2020; accepted December 10, 2020. Date of publication December 15, 2020; date of current version April 9, 2021. This work was supported by the American University of Sharjah under a Faculty Research Grant no. FRG20-M-E10. The work of Ahmed S. Ibrahim was supported in part by the National Science Foundation under Award CNS-1816112. The associate editor coordinating the review of this letter and approving it for publication was H. Tabassum. *(Corresponding author: Mahmoud H. Ismail.)*

Mai Kafafy is with the Department of Electronics and Communications Engineering, Faculty of Engineering, Cairo University, Giza 12613, Egypt (e-mail: mai.b.s.ali@eng.cu.edu.eg).

Ahmed S. Ibrahim is with the Electrical and Computer Engineering Department, Florida International University, Miami, FL 33174 USA (e-mail: aibrahim@fiu.edu).

Mahmoud H. Ismail is with the Department of Electrical Engineering, American University of Sharjah, Sharjah, United Arab Emirates, and also with the Department of Electronics and Communications Engineering, Faculty of Engineering, Cairo University, Giza 12613, Egypt (e-mail: mhibrahim@aus.edu).

Digital Object Identifier 10.1109/LCOMM.2020.3045060

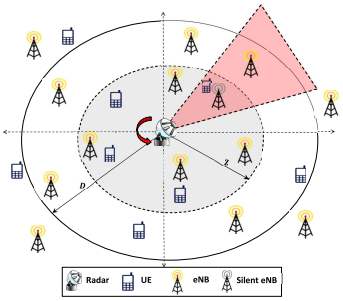

Fig. 1. A cellular system in the vicinity of a rotating radar with guard zone.

the guard zone and when it is not allowed. This enables us to derive a closed-form expression for the improvement in the cellular coverage as a result of allowing spatial opportunistic spectrum sharing inside the guard zone.

II. System Model

We consider a radar surrounded by eNBs as shown in Fig. 1. The eNBs are located randomly in space according to a Homogeneous Poisson Point Process (HPPP) Φ_c with density ζ_c and they use the radar spectrum as a supplement to their licensed spectrum (similar to LTE-Unlicensed [8]). The radar has a guard zone of radius Z and the eNBs inside this zone should synchronize their transmission with the radar rotation such that they only share the radar spectrum when outside the radar beam. This can be done by spectrum sensing or by monitoring the radar rotation pattern [1], [4]. eNBs outside the guard zone, however, use the radar spectrum all the time without synchronization, but subject to constraints on their total interference. We assume that cellular User Equipment (UE) are randomly located also according to an HPPP Φ_u with density ζ_u. All eNBs and UEs are assumed to have omnidirectional antennas and a typical UE is served by its nearest eNB. An eNB serves its associated users orthogonally with a downlink power P_c such that there is no intra-cell interference, but inter-cell interference still exists. Without loss of generality, we consider a circular region of interest (the white circle in Fig. 1). The circle center (i.e., the origin) is the radar position and its radius is the radar range (D).

We also consider a monostatic rotating horizontal search radar, which uses a Constant False Alarm Rate (CFAR) detector that keeps the probability of false alarm, denoted by P_{FA}, fixed by adjusting the detection threshold according to the estimated interference [9]. CFAR detectors are important as radars are usually designed to tolerate certain P_{FA} since higher false alarm rates overload the radar and drain its resources. The relation between the average P_{FA}, the probability of detection P_D, and the Signal to Interference and Noise Ratio (SINR) of a CFAR detector is $P_D = \left[1 + \left(P_{FA}^{\frac{-1}{N}} - 1\right) / (1 + \text{SINR}_r)\right]^{-N}$ [9], where N is the number of range bins used to estimate the interference power. SINR_r is the SINR at the radar given as follows [9]

$$\text{SINR}_r = \frac{n_p P_t G_t G_r \lambda^2 \sigma}{(4\pi)^3 D^4 (\sigma_n^2 + I_{c\to r})}, \tag{1}$$

where P_t, λ, σ and n_p represent the radar transmission power, its signal wavelength, the cross section of the target, and the number of coherently processed pulses, respectively. Also, $\sigma_{n,r}^2$ and $I_{c\to r}$ are the thermal noise and downlink cellular interference powers at the radar, respectively. Finally, G_t and G_r are the transmit and receive antenna gains where we assume $G_t = G_r = G$. The radar antenna is also assumed to have a perfect radiation pattern such that

$$G(\theta) = \begin{cases} G_{max}, & \Theta_B - \frac{\Theta_3}{2} \le \theta \le \Theta_B + \frac{\Theta_3}{2}, \\ 0, & \text{otherwise}, \end{cases} \tag{2}$$

where Θ_B and Θ_3 are the direction of the radar beam and its beamwidth. Since eNBs inside the guard zone remain silent when in the radar beam, only eNBs outside the guard zone contribute to $I_{c\to r}$ as follows

$$\begin{aligned} I_{c\to r} &= \mathbb{E}_{h,\Phi_c}\left[\sum_{i\in\Phi_c} h_i P_c G_r(\theta_i) d_i^{-\alpha}\right] \\ &\overset{a}{=} P_c \zeta_c \int_{\theta=-\pi}^{\pi} G_r(\theta) d\theta \int_{r=Z}^{\infty} \frac{r dr}{r^\alpha} = \frac{P_c \zeta_c G_{max} \Theta_3 Z^{2-\alpha}}{\alpha - 2}. \end{aligned} \tag{3}$$

The variables d_i, θ_i, and h_i are the distance, the azimuth angle, and the channel power gain between the radar and eNB $i \in \Phi_c$ and α is the pathloss exponent. We assume small scale Rayleigh fading such that $h_i \sim \exp(1)$ are i.i.d. The $\overset{a}{=}$ in (3) is from Campbell's theorem [10] and because h_i are i.i.d. with $\mathbb{E}_h[h] = 1$. It is worth mentioning that the interference in (3) is a worst case interference as we assume all eNBs to be active.

As seen from (1) and (3), the presence of a cellular system that shares the radar spectrum affects the radar performance through three parameters: the eNB power P_c, the eNB density ζ_c, and the guard zone size Z. The values of P_c, ζ_c, and Z should be chosen such that $I_{c\to r}$ is below some threshold I_{th}. From (1) and (3), the following constraint should be satisfied

$$\frac{P_c \zeta_c}{Z^{\alpha-2}} \le \frac{(\alpha-2) I_{th}}{G_{max} \Theta_3}, I_{th} = \frac{n_p P_t G_{max}^2 \lambda^2 \sigma}{(4\pi)^3 D^4 \text{SINR}_{r,th}} - \sigma_{n,r}^2, \tag{4}$$

where $\text{SINR}_{r,th}$ is the SINR required for specific detection and false alarm probabilities. On the other hand, it is also important to analyze the performance of the cellular system in the presence of the radar and under the interference constraint in (4). To that end, in the next section, we define and formulate the cellular probability of coverage in terms of the radar operation parameters, the eNBs operation parameters, the guard zone size, and the user density.

III. Cellular System Performance

Consider a UE located at distance u from the radar and r_0 from its serving eNB. Due to the radar's rotation and the azimuth symmetry of the network, we assume, without loss of generality, that the UE is located at $\theta = 0^\circ$. The SINR at the UE is thus

$$\text{SINR} = \frac{P_c h_0 r_0^{-\alpha}}{\sigma_{n,c}^2 + I_{r\to u} + I_{c\to u}}, \tag{5}$$

where $h_0 \sim \exp(1)$ is the serving eNB-UE channel power gain, $\sigma_{n,c}^2$ is the noise power at the UE and $I_{r\to u}$ is the radar

interference at the UE. From (2), $I_{r\to u}$ is non-zero only when the UE is in the radar's beam as follows,

$$I_{r\to u} = \bar{P}_t u^{-\alpha} G_{max}, \quad \Theta_B \in [-\Theta_3/2, \Theta_3/2], \tag{6}$$

where $\bar{P}_t = P_t \nu T_p$ is the average radar transmit power with T_p being the transmit pulse duration and ν being the pulse repetition frequency. In (5), $I_{c\to u} = P_c \sum_{i\in\Phi_I} h_i d_i^{-\alpha_i}$ is the downlink cellular interference at the UE, where Φ_I is the set of active interfering eNBs and h_i and d_i are the channel power gain and distance between the UE and eNB $i \in \Phi_I$, respectively. The probability of coverage is the probability that the SINR of a typical UE exceeds a threshold γ_c. The conditional probability of coverage is

$$\begin{aligned}
&P(\text{SINR} \geq \gamma_c | r_0, u, \Theta_B) \\
&\stackrel{a}{=} \mathbb{E}_{\Phi_I,h}\left[P\left(h_0 \geq \frac{r_0^\alpha \gamma_c}{P_c}\left[\sigma_{n,c}^2 + I_{r\to u} + I_{c\to u}\right]\right)\right] \\
&\stackrel{b}{=} \exp\left(-\frac{\gamma_c r_0^\alpha}{P_c}\left(\sigma_{n,c}^2 + I_{r\to u}\right)\right)\mathbb{E}_{\Phi_I,h}\left[\exp\left(-\frac{\gamma_c r_0^\alpha I_{c\to u}}{P_c}\right)\right], \\
&\stackrel{c}{=} \exp\left(-\frac{\gamma_c r_0^\alpha}{P_c}\left(\sigma_{n,c}^2 + I_{r\to u}\right)\right)\mathbb{E}_{\Phi_I}\left[\prod_{i\in\Phi_I}\frac{1}{1+\gamma_c\left(\frac{r_0}{d_i}\right)^\alpha}\right] \\
&\stackrel{d}{=} \exp\left(-\frac{\gamma_c r_0^\alpha}{P_c}\left(\sigma_{n,c}^2 + I_{r\to u}\right) - \zeta_c P(\text{active})\left[\Im_1 - \Im_2\right]\right)
\end{aligned} \tag{7}$$

where $\stackrel{a}{=}$ is by substituting with SINR from (5), $\stackrel{b}{=}$ is because $h_0 \sim \exp(1)$, $\stackrel{c}{=}$ is from substituting with $I_{c\to u}$ and knowing that $h_i \sim \exp(1)$ are i.i.d., $\stackrel{d}{=}$ is from the Probability Generating Functional (PGFL) of the HPPP [10] and $P(\text{active}) = 1 - \left(1 + \frac{\zeta_u}{3.5\zeta_c}\right)^{-3.5}$ is the probability of the eNB being active [11]. In (7), $\Im_1$ is the integration over all the interfering eNBs given by [10]

$$\Im_1 = \int_{r=r_0}^{\infty}\int_{\theta=-\pi}^{\pi} \frac{\gamma_c r}{\gamma_c + \left(\frac{r}{r_0}\right)^\alpha} dr d\theta = \int_{r=r_0}^{\infty} \frac{2\pi\gamma_c r}{\gamma_c + \left(\frac{r}{r_0}\right)^\alpha} dr. \tag{8}$$

Unlike regular cellular systems, the eNBs inside the radar guard zone remain silent when in the radar beam, so these need to be excluded from the set Φ_I through the subtraction of the term $\Im_2$ in (7) as follows

$$\Im_2 = \iint \frac{\gamma_c r}{\gamma_c + \left(\frac{\sqrt{r^2+u^2-2ru\cos(\theta)}}{r_0}\right)^\alpha} dr d\theta. \tag{9}$$

The integration in (9) is over the grey region in Fig. 2(a) (i.e., the silent part of the guard zone), which is defined by the constraints $0 \leq r \leq Z$ and $\Theta_B - \Theta_3/2 \leq \Theta \leq \Theta_B + \Theta_3/2$ besides the constraint $\sqrt{r^2+u^2-2ru\cos(\theta)} \geq r_0$ as interfering eNBs should be farther from the serving eNB of the UE. Also, unlike regular cellular networks, the probability of coverage at position u is affected by whether a UE at this position is served by an eNB inside or outside the guard zone. Specifically, if the UE is served by an eNB inside the guard zone, the eNB will go silent every time the radar beam passes through it. From Fig. 2(b), the probability that a UE at u is served by an eNB inside the radar guard zone given r_0 is

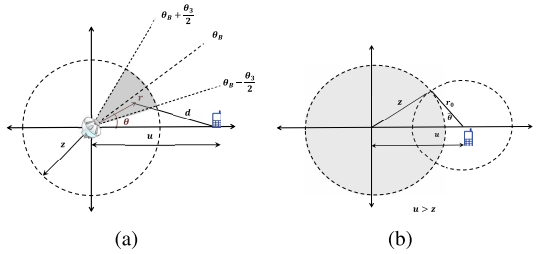

Fig. 2. (a) Subtracting the interference of silent eNBs in the grey region, (b) A UE at u can be served by an eNB inside or outside the radar guard zone.

$$\begin{aligned}
&P(\text{in}|u, r_0) \\
&= \begin{cases} 1(u < Z), & 0 \leq r_0 \leq |u - Z|, \\ \frac{1}{\pi}\cos^{-1}\left(\frac{u^2+r_0^2-Z^2}{2ur_0}\right), & |u-Z| \leq r_0 \leq u+Z, \\ 0, & r_0 \geq u+Z, \end{cases}
\end{aligned} \tag{10}$$

where $1(u < Z)$ is 1 if $u < Z$ and 0 otherwise. To show the effect of the eNB density on the probability that a UE at u is served by an eNB inside the guard zone, we calculate $P(\text{in}|u)$ by averaging (10) over r_0 whose Probability Density Function (PDF) is $f_{r_0}(r_0) = 2\pi\zeta_c r_0 \exp(-\zeta_c \pi r_0^2)$ [10]. Using the approximation $\cos^{-1}(x) \approx \pi/2 - x$ yields

$$\begin{aligned}
P(\text{in}|u) \approx\ &\beta(u+Z) - \beta(|u-Z|) \\
&+(1 - e^{-\pi\zeta_c(Z-u)^2})1(u < Z),
\end{aligned} \tag{11}$$

where $\beta(x) = \frac{e^{-\pi\zeta_c x^2}}{2}\left(\frac{x}{\pi u} - 1\right) - \frac{1}{2u}\text{erf}\left(x\sqrt{\pi\zeta_c}\right) \times \left[\frac{1}{2\pi\sqrt{\zeta_c}} + \sqrt{\zeta_c}(u^2 - Z^2)\right]$. Since the radar antenna rotates periodically and the UEs positions follow an HPPP then the PDFs of Θ_B and u are $f_{\Theta_B}(\Theta_B) = \frac{1}{2\pi}, \Theta_B \in [-\pi, \pi]$ and $f_u(u) = \frac{2u}{D^2}, u \in [0, D]$, respectively. Now, the probability of coverage can be obtained by combining (7) and (10) and averaging over r_0, Θ_B and u using their PDFs as follows

$$\begin{aligned}
&P(\text{coverage}) \\
&= \frac{2\zeta_c}{D^2}\int_{u=0}^{D} u \int_{r_0=0}^{\infty} r_0 \exp\Big(-\zeta_c\left(\pi r_0^2 + P(\text{active})\Im_1\right) \\
&\quad - \frac{\gamma_c r_0^\alpha \sigma_{n,c}^2}{P_c}\Big)\Big[\int_{\Theta_B \notin [-\frac{\Theta_3}{2}, \frac{\Theta_3}{2}]} \exp\left(\zeta_c P(\text{active})\Im_2\right) d\Theta_B \\
&\quad + (1 - P(\text{in}|u, r_0)) \\
&\quad \int_{\Theta_B \in [\frac{\Theta_3}{2}, \frac{\Theta_3}{2}]} \exp\left(-\frac{\gamma_c r_0^\alpha \bar{P}_t u^{-\alpha} G_{max}}{P_c} + \zeta_c P(\text{active})\Im_2\right) d\Theta_B\Big] \\
&\quad \times dr_0 du.
\end{aligned} \tag{12}$$

The integral on the second line handles the case when the UE (and presumably its serving eNB) are not in the radar beam (i.e., $G_t(0) = 0$) while that on the third line handles the case when the UE and its eNB are in the radar beam (i.e., $G_t(0) = G_{max}$). In the latter case, the UE will be served on the radar spectrum only if its serving eNB lies outside the guard zone, which accounts for the factor $(1 - P(\text{in}|u, r_0))$.

If spectrum sharing is not allowed inside the guard zone, all eNBs inside the guard zone will be silent all the time regardless of their relative position to the radar beam. This means that the two integrals over Θ_B in (12) would be multiplied by $(1-P(\text{in}|u,r_0))$ to reflect the fact that the UE will be served only if it is associated to an eNB outside the guard zone as follows

$$P(\text{coverage}|\text{silent}) = \frac{2\zeta_c}{D^2}\int_{u=0}^{D} u \int_{r_0=0}^{\infty} r_0 \exp\Bigg(-\zeta_c\Bigg(\pi r_0^2 + P(\text{active})\Im_1\Bigg) - \frac{\gamma_c r_0^{\alpha}\sigma_{n,c}^2}{P_c}\Bigg)(1-P(\text{in}|u,r_0))\Bigg[\int_{\Theta_B\notin[-\frac{\Theta_3}{2},\frac{\Theta_3}{2}]} \exp\left(\zeta_c P(\text{active})\Im_2\right) d\Theta_B + \int_{\Theta_B\in[\frac{\Theta_3}{2},\frac{\Theta_3}{2}]} \exp\Bigg(\zeta_c P(\text{active})\Im_2 - \frac{\gamma_c r_0^{\alpha}\bar{P}_t u^{-\alpha} G_{max}}{P_c} + \Bigg) d\Theta_B\Bigg] dr_0 du. \quad (13)$$

It is worth mentioning that $\Im_2$ in (13) is the same as $\Im_2$ in (9), but the integration over θ is from $-\pi$ to π because all eNBs inside the guard zone are now assumed silent. Clearly, (12) and (13) are complicated to evaluate, hence, in the following theorem, we find alternative closed form approximations for them under some simplifying assumptions.

Theorem 1: The probabilities of coverage in (12) *and* (13) *have the following closed forms*

$$P(\text{coverage}) \approx \frac{\zeta_c(2\pi-\Theta_3)}{2\sqrt{2b+a^2}} + \psi, \quad (14a)$$

$$P(\text{coverage}|\text{silent}) \approx \frac{\zeta_c(2\pi-\Theta_3)}{2\sqrt{2b+a^2}}\left(1-\frac{Z^2}{D^2}\right) + \psi, \quad (14b)$$

where $a = \zeta_c\pi(1+P(\textit{active})\sqrt{\gamma_c}\tan^{-1}\sqrt{\gamma_c})$, $b = \frac{\gamma_c\sigma_{n,c}^2}{P_c}$, $\psi = \frac{\zeta_c\Theta_3\left[\sqrt{D^4(2b+a^2)+2c}-\sqrt{Z^4(2b+a^2)+2c}\right]}{2D^2(2b+a^2)}$ *and* $c = \frac{\gamma_c\bar{P}_t G_{max}}{P_c}$ *in the special case that* $\alpha = 4$ *and under the following assumptions: 1)* ζ_c *is high enough such that* $P(in|u,r_0)\approx 1$ *if* $u < Z$ *and 0 otherwise and 2) The reduction in the interference observed by the UE due to the silent eNBs inside the radar beam is neglected (i.e.,* $\Im_2 \approx 0$*).*

Proof: From [10], $\Im_1 = \pi r_0^2\sqrt{\gamma_c}\tan^{-1}(\sqrt{\gamma_c})$. Substituting in (12) using the above assumptions yields

$$P(\text{coverage}) = \frac{2\zeta_c}{D^2}\int_{u=0}^{D}\int_{r_0=0}^{\infty} u r_0 \exp\Bigg(-\zeta_c\pi r_0^2\Bigg(1 + P(\text{active})\sqrt{\gamma_c}\tan^{-1}(\sqrt{\gamma_c})\Bigg) - \frac{\gamma_c\sigma_{n,c}^2}{P_c}r_0^4\Bigg)\Bigg[(2\pi-\Theta_3) + 1(u\geq Z)\Theta_3\exp\left(-\frac{\gamma_c\bar{P}_t G_{max}}{P_c u^4}r_0^4\right)\Bigg] dr_0 du. \quad (15)$$

The above equation can be rewritten as $T_1 + T_2$, where T_1 is

$$T_1 = (2\pi-\Theta_3)\frac{2\zeta_c}{D^2}\int_{u=0}^{D} u du \int_{r_0=0}^{\infty} r_0\exp(-ar_0^2 - br_0^4)dr_0 \stackrel{a}{=} \zeta_c(2\pi-\Theta_3)\frac{1}{2\sqrt{2b+a^2}}, \quad (16)$$

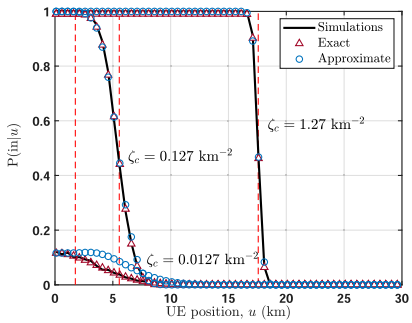

Fig. 3. The probability of being served by an eNB inside the radar guard zone versus the UE position for different eNB densities (at $\Theta_3 = 90°$).

where $\stackrel{a}{=}$ follows from executing the integral and using the approximation $Q(x)\approx\frac{1}{\sqrt{2\pi}}\frac{\exp(-x^2/2)}{\sqrt{1+x^2}}$ and the term T_2 is

$$T_2 = \int_{u=Z}^{D}\int_{r_0=0}^{\infty}\frac{2\zeta_c\Theta_3 u r_0}{D^2}\exp\left(-ar_0^2 - \left(b+cu^{-4}\right)r_0^4\right)dr_0 du \stackrel{a}{=} \frac{\zeta_c\Theta_3\left[\sqrt{D^4(2b+a^2)+2c}-\sqrt{Z^4(2b+a^2)+2c}\right]}{2D^2(2b+a^2)}, \quad (17)$$

where $\stackrel{a}{=}$ follows from the integration over r_0 using the same approach in (16). Equation (14b) can be proved by applying the same mathematical approach on (13) □

In the next section, we will show that the closed form expressions obtained above are almost indistinguishable from the cumbersome exact ones. Finally, one can quantify the improvement in coverage due to opportunistic sharing inside the guard zone by subtracting (14b) from (14a) and substituting with Z from (4) to yield

$$\text{coverage improvement} \approx \frac{PcG_{max}\zeta_c^2\Theta_3(2\pi-\Theta_3)}{4D^2 I_{th}\sqrt{2b+a^2}}. \quad (18)$$

IV. Numerical and Simulation Results

Figure 3 shows the probability that a UE at u is served by an eNB inside the guard zone for different eNB densities, ζ_c. All figures are generated using the simulation parameters in Table I [12]. The exact probability is calculated by averaging (10) over r_0, while its approximation is calculated from (11). The vertical dashed lines mark the guard zone radius Z calculated using (4) for each ζ_c at $\Theta_3 = 90°$. As shown in the figure, a denser eNB deployment requires a wider guard zone. At low ζ_c, only few eNBs lie inside the guard zone, so the chances of being served by an eNB inside the guard zone is low even for UEs located inside the guard zone. As ζ_c increases, the probability that a UE inside (outside) the guard zone be served by an eNB inside (outside) the guard zone increases. However, there still exists an uncertainty for UEs at the edge of the guard zone. This uncertainty decreases as ζ_c increases.

Figure 4 sketches the cellular probability of coverage vs. the radar beamwidth on the bottom x-axis (with ζ_c =1.27 Km^{-2}). The top axis shows the guard zone radius calculated from (4) for each beamwidth. The figure considers the two cases when spatial opportunistic spectrum sharing is allowed inside the guard zone, and when it is not allowed inside the guard

TABLE I
SIMULATION PARAMETERS

Radar parameters	
Radar wavelength (λ)	0.0833 m
Radar antenna power gain (G_{max})	32 dB
Pulse repetition frequency (ν)	1.1 kHz
Pulse width (T_P)	0.9 μs
Radar cross section (σ)	100
Number of points in interference estimation (N)	20
Radar transmission power (P_t)	850 kW
Radar range (D)	50 km
Number of coherently processed pulses (n_p)	1100
False alarm and detection probabilities (P_{FA} and P_D)	1×10^{-4}, 0.8
Cellular parameters	
eNB transmission power (P_c)	43 dBm
eNB antenna power gain	14 dB
cellular SINR threshold (γ_c)	5 dB
pathloss exponent (α)	4
UE density (ζ_u)	0.127 km^{-2}

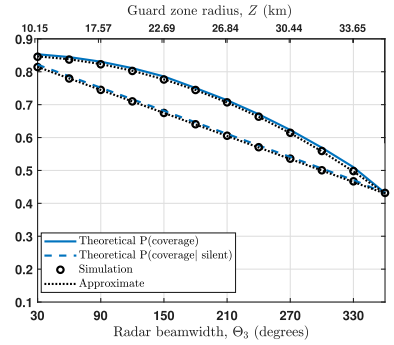

Fig. 4. The probability of coverage versus the radar beamwidth for hybrid sharing and strictly silent guard zones (with ζ_c =1.27 km^{-2}).

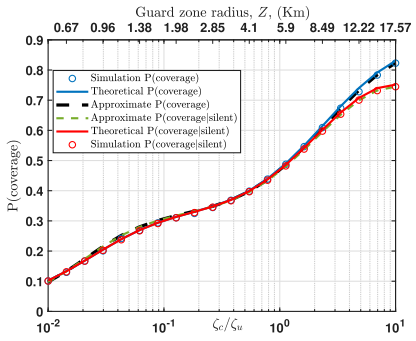

Fig. 5. The probability of coverage versus the ratio between the eNBs to UE densities for hybrid sharing and strictly silent guard zones (at $\Theta_3 = 90°$).

zone. The theoretical probabilities of coverage for the two cases are obtained from (12), (13) and the approximate ones from (14a), (14b). Clearly, the probability of coverage decreases as Θ_3 increases since the guard zone gets bigger, more eNBs in the guard zone lie inside the radar beam, and the radar interference affects wider spatial sections outside the guard zone. The figure also shows that allowing opportunistic sharing in the guard zone generally improves the probabilities of coverage. However, the improvement is small at $\Theta_3 = 30°$ due to the small size of the guard zone and it is also small at $\Theta_3 = 330°$ because the eNBs inside the guard zone are silent most of the time due to the wide radar beamwidth. Also, the two cases have the same performance at $\Theta_3 = 360°$ because, in both cases, eNBs inside the guard zone are silent as they are always inside the radar beam. The effect of Θ_3 on the coverage gain can also be verified from (18). Similarly, Fig. 5 sketches the probability of coverage versus the ratio of the eNBs to UE densities at $\Theta_3 = 90°$. Clearly, increasing ζ_c improves the probability of coverage as the UEs get closer to their serving eNBs. Also, allowing opportunistic sharing in the guard zone improves the coverage at high ζ_c, which can be verified from (18) as more eNBs in the guard zone can use the radar spectrum. Finally, Figs. 4 and 5 confirm the accuracy of the proposed closed form approximations as well.

V. CONCLUSION

This letter presented a stochastic geometry based analysis of the performance of a cellular system sharing spectrum with a rotating radar. Results showed the benefits of allowing spatial opportunistic spectrum sharing compared to a strictly silent guard zone. The analysis could be extended to include the effect of imperfect radar radiation pattern and imperfect synchronization between eNBs transmission and radar rotation.

REFERENCES

[1] M. Labib, V. Marojevic, A. F. Martone, J. H. Reed, and A. I. Zaghloui, "Coexistence between communications and radar systems: A survey," *URSI Radio Sci. Bull.*, vol. 2017, no. 362, pp. 74–82, Sep. 2017.
[2] H. Wang, J. T. Johnson, and C. J. Baker, "Spectrum sharing between communications and ATC radar systems," *IET Radar, Sonar Navigat.*, vol. 11, no. 6, pp. 994–1001, Jun. 2017.
[3] M. Ghorbanzadeh, E. Visotsky, P. Moorut, and C. Clancy, "Radar interference into LTE base stations in the 3.5 GHz band," *Phys. Commun.*, vol. 20, pp. 33–47, Sep. 2016.
[4] R. Saruthirathanaworakun, J. M. Peha, and L. M. Correia, "Opportunistic sharing between rotating radar and cellular," *IEEE J. Sel. Areas Commun.*, vol. 30, no. 10, pp. 1900–1910, Nov. 2012.
[5] N. N. Krishnan, R. Kumbhkar, N. Mandayam, I. Seskar, and S. Kompella, "Coexistence of radar and communication systems in CBRS bands through downlink power control," in *Proc. IEEE MILCOM*, May 2017, pp. 713–718.
[6] M. Labib, A. Martone, V. Marojevic, J. Reed, and A. Zaghloul, "A stochastic optimization approach for spectrum sharing of radar and LTE systems," *IEEE Access*, vol. 7, pp. 60814–60826, 2019.
[7] F. Hessar and S. Roy, "Spectrum sharing between a surveillance radar and secondary WiFi networks," *IEEE Trans. Aerosp. Electron. Syst*, vol. 52, no. 3, pp. 1434–1448, Aug. 2016.
[8] H.-J. Kwon *et al.*, "Licensed-assisted access to unlicensed spectrum in LTE Release 13," *IEEE Commun. Mag.*, vol. 55, no. 2, pp. 201–207, Feb. 2017.
[9] M. Richards, J. Scheer, W. Holm, and W. Melvin, *Principles of Modern Radar: Basic Principles*. New York, NY, USA: SciTech, 2010.
[10] J. G. Andrews, A. K. Gupta, and H. S. Dhillon, "A primer on cellular network analysis using stochastic geometry," 2016, *arXiv:1604.03183*. [Online]. Available: http://arxiv.org/abs/1604.03183
[11] S. M. Yu and S.-L. Kim, "Downlink capacity and base station density in cellular networks," in *Proc. IEEE WiOpt*, Dec. 2013, pp. 119–124.
[12] J. H. Reed *et al.*, "On the co-existence of TD-LTE and radar over 3.5 GHz band: An experimental study," *IEEE Wireless Commun. Lett.*, vol. 5, no. 4, pp. 368–371, Aug. 2016.